


Article

Aspects Regarding the Optimization of Cross Geometry in Traction Asynchronous Motors Using the Theory of Nonlinear Circuits

Sorin Enache , Ion Vlad and Monica Adela Enache

Electrical Engineering Faculty of Craiova, University of Craiova, 200585 Craiova, Romania

* Correspondence: senache@em.ucv.ro

Abstract: Modern electrical traction uses asynchronous motors for driving railway vehicles because these motors have a lot of advantages in comparison with the classical, direct current motors. Reducing active and reactive electrical energy consumption is a concern in the case of these motors, meaning a decrease in exploitation costs. The research carried out shows, by results and simulations, the effects of the geometry optimization for the stator and rotor lamination and emphasizes how much the total and exploitation costs. Cross geometry optimization means preserving constant electromagnetic stresses, using the same gauge dimensions, preserving the constant ampere-turn for a pole pair, having a maximum torque exceeding the imposed limit, and increasing the air-gap magnetic induction. The results obtained indicate a decrease in the total cost, by 42,600 € (12.31%), for a asynchronous traction motor in comparison with the existing variant.

Keywords: asynchronous motors for railway traction; optimal design; simulations



Citation: Enache, S.; Vlad, I.; Enache, M.A. Aspects Regarding the Optimization of Cross Geometry in Traction Asynchronous Motors Using the Theory of Nonlinear Circuits. *Energies* **2022**, *15*, 6648. <https://doi.org/10.3390/en15186648>

Academic Editors: Ioana-Gabriela Sirbu and Lucian Mandache

Received: 27 July 2022

Accepted: 8 September 2022

Published: 11 September 2022

Publisher's Note: MDPI stays neutral with regard to jurisdictional claims in published maps and institutional affiliations.



Copyright: © 2022 by the authors. Licensee MDPI, Basel, Switzerland. This article is an open access article distributed under the terms and conditions of the Creative Commons Attribution (CC BY) license (<https://creativecommons.org/licenses/by/4.0/>).

1. Introduction

In electrical railway vehicles, the limitations imposed by the railway gauge and the diameter of the rolling wheel restrict the possibilities of choosing the geometrical dimensions of both the transmission and electrical traction motor, even in the design stage.

That is why, when designing the traction motor, the limited gauge dimensions, the mechanical stresses, and the vibrations transmitted from the track, as well as the electrical stresses caused by the variation of the load during the movement of the train and the specific power supply conditions, are taken into account [1,2].

Consequently, in order to finalize the solution regarding electrical traction motor suspension and the transmission of the motor torque to the axle, a series of requirements are needed:

- Electrical traction motors should be placed so that they are easily accessible for verifications, revisions, and repairs;
- The transmission should enable the rotor to rotate faster than the motor axle is driven, ensuring the optimum speed of the electrical traction motor.

Power electronics have changed the traction system, enabling it to carry out electrical transmission with asynchronous motors, both for diesel and electrical traction, Figure 1 [3–5]. As a result, it increases the power installed on a vehicle, the reliability of the traction motor, the overload capacity, etc.

The authors of this paper have studied a lot of railway traction motors (direct current and asynchronous), have published papers in magazines and specialized conferences, and are concerned with optimizing their design and construction.

The current research carried out presents the effects of optimizing the geometry of the stator and rotor plates, and shows how manufacturing, operating, and total costs decrease.

To justify the result of optimizing the transverse geometry, an asynchronous motor from an electric locomotive manufactured in Romania was used as an example, the electrical

demands were kept constant (so as not to influence the heating), and the maximum torque, gauge dimensions, and cost reduction were followed.



Figure 1. Electrical locomotive.

2. Analysis of Stator and Rotor Slot Geometry

If the total number of conductors in a slot is n_{c1} , the number of stator parallel current ways is a_1 , the slot filling factor is k_u , and the stator winding conduction current density is J_1 , the needed section of the slot can be established as follows:

$$S_{c1} = \frac{1}{k_u} \cdot \frac{I_{1N} \cdot n_{c1}}{a_1 J_1} \quad (1)$$

In asynchronous motors, the magnetization current is also defined as a percentage of the rated current in order to quantify the reactive power consumption. It is known that this percentage quantity, $i_{1\mu}$, is high in machines having a lot of poles.

$$i_{1\mu} = \frac{I_{1\mu}}{I_{1N}} \quad (2)$$

From (1) and (2), the following is obtained:

$$S_{c1} = \frac{1}{k_u} \cdot \frac{I_{1\mu}}{i_{1\mu}} \cdot \frac{n_{c1}}{a_1 J_1} = \frac{1}{k_u a_1 i_{1\mu} J_1} (n_{c1} I_{1\mu}) \quad (3)$$

and finally, from (3) it follows:

$$S_{c1} = \frac{1}{k_u a_1 i_{1\mu} J_1} \cdot \vartheta_{c1} \quad (4)$$

where ϑ_{c1} is the total magnetization ampere-turn corresponding to a stator slot.

The values ϑ_{c1} can be also established from the current load (A) by knowing the tooth pitch (t_1), finally resulting in:

$$S_{c1} = \frac{1}{k_u a_1 i_{1\mu} J_1} \cdot A t_1 \quad (5)$$

In the optimization problem analyzed, the quantities k_u , $i_{1\mu}$, and a_1 , are considered as constant and known and A and J_1 are the electrical stresses of the machine.

This analysis concerns the influence of the stator, respectively, rotor slot dimensions upon the air-gap magnetic induction. It is aimed at establishing some optimum values in the case of the variables $\beta_{c1} = h_{c1}/b_{c1}$ and $\beta_{c2} = h_{c2}/b_{c2}$ (b_{c1} , h_{c1} —the width and height of the stator notch, respectively, and b_{c2} , h_{c2} for the rotor), in order to obtain a maximum air-gap magnetic induction without modifying the outer diameter of the stator lamination and the magnetic core length.

This optimization takes into account that the total ampere-turn, for a pole pair, is a known constant quantity (the field source $\vartheta = \text{const.}$) [6–9]. The anisotropic model of the

electrical machine enables establishing the air-gap magnetic induction, according to the known design method.

Variables Defining the Cross Geometry of an Asynchronous Motor

According to the known geometry of the stator and rotor lamination, the following variables are used (Figure 2) which establish the essence of asynchronous motor cross geometry:

- D_e, D —outer and inner diameter, respectively, of the stator lamination;
- $D-2\delta, D_i$ —outer and inner diameter, respectively, of the rotor lamination;
- D_1, D_2 —diameters of the slot base, for the stator and rotor slot, respectively;
- S_{c1}, S_{c2} —areas of the geometric surfaces, for the stator and rotor slot, respectively;
- δ —machine air-gap.

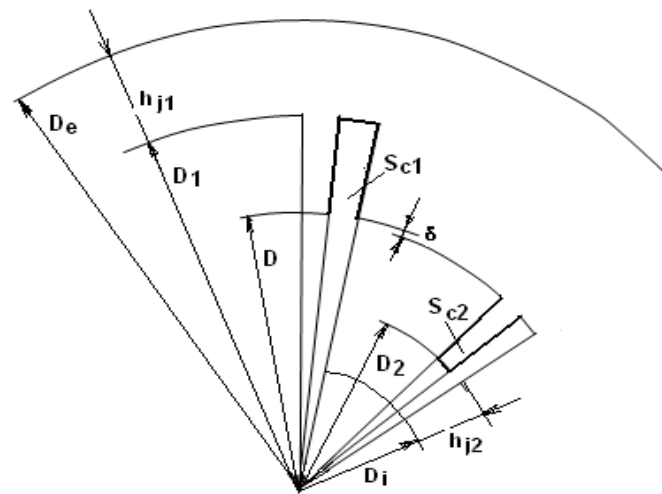


Figure 2. Notations used in cross geometry.

3. The Simplified Mathematical Model Used to Optimize the Transverse Geometry of the Asynchronous Motor

By using the anisotropic model of the field and by adopting, in all situations, the maximization criterion of magnetic induction, B , the possibilities of the optimization of the cross geometry of an asynchronous machine with constant air-gap are analyzed [10–12].

The cross geometry optimization has taken the following aspects into consideration:

- The outer diameter of the stator plate is kept for the analyzed motor;
- The solenacy corresponding to the magnetizing current (the magnetomotive voltage on a pair of poles), in the study being done, will be an imposed quantity (the reference solenacy);
- The same electrical stresses are preserved;
- The constant air-gap is preserved, the same one as in the analyzed motor;
- The geometric dimensions in the cross geometry and the magnetic stresses in all parts of the magnetic circuit are modified so that the total ampere-turn, for a pole pair, is minimized;
- For these dimensions of the magnetic circuit, the air-gap magnetic induction is progressively increased (so the inductances in the teeth and yokes also increase, etc.), and as a result, solenacy on the pair of poles increases until the imposed value of “reference solenacy” is reached.

In this way, if the total length of the engine is kept, then in the same dimensions, the engine power can be increased. Another possibility is to keep the power requested by the beneficiary, resulting in a shorter engine length.

In this paper, the option of optimizing the transversal geometry at the power requested by the beneficiary was used. The results of this analysis are further presented through simulations, in several distinct stages.

3.1. Objective Function

We aim at optimizing the cross-section of asynchronous motors used in an electrical locomotive. Optimization is aimed at maximizing the air-gap magnetic induction. The results of this analysis are further presented through simulations, in several distinct stages, until the solenation on the pair of poles reaches the “reference value” while keeping the same gauge dimensions [13–16].

That is why we impose the minimum total cost as a criterion, $f(\mathbf{x}) = C_t = \min.$, because it reflects correctly the investment made for acquiring this motor, C_f , as well as the exploitation costs, C_e , necessary during the investment damping:

$$C_t = C + C_e \quad (6)$$

For C_f , the fabrication cost of the motor, we have the relation:

$$C_f = k_f C_{ma} \quad (7)$$

After designing the asynchronous motor, the amounts of active materials used are known, so it is possible to establish the cost of the active materials, C_{ma} . By using a factor k_f , established for asynchronous motors of a similar type, it is possible to consider the costs afferent to technological manufacturing processes and workmanship, and different costs specific to the manufacturing company.

The exploitation cost can be computed by the relation:

$$C_e = C_{ea} + C_{er} = N_o T_{ri} c_{el.a} \Sigma p + N_o T_{ri} c_{el.r} \Sigma q \quad (8)$$

C_{ea}/C_{er} are the cost of consumed active/reactive electricity, N_o is the number of hours of operation in a year of the engine, $c_{el.a}/c_{el.r}$ are the cost of one kWh of active electricity and the cost of a kVARh, respectively, T_{ri} is the investment recovery time in years, Σp are the total losses in the motor, and Σq is the reactive energy consumption.

3.2. Variables and Restrictions of the Objective Function

The study regarding the optimization uses four main variables presented before: D is the inner stator diameter, β_{c1}/β_{c2} are the shape factors for stator/rotor slots, and D_{ir} is the inner diameter of rotor lamination.

The mathematical model used in the design takes the following variable restrictions into account:

$$\begin{aligned} x_{\min_i} &\leq x_i \leq x_{\max_i} \\ x_i &= \{D, \beta_{c1}, \beta_{c2}, D_{ir}\} \end{aligned} \quad (9)$$

The customer imposed the following requirements for traction motors used in electrical locomotive:

$$D_e \leq D_{e.i}; \quad L_e \leq L_{e.i}; \quad m_m \geq m_{m.i} \quad (10)$$

D_e, L_e, m_m —gauge dimensions (D_e is the outer diameter and L_e is the total length of the motor) and $m_m = M_m/M_N$ —maximum torque, per unit values.

4. Simulated Results

The research carried out for optimizing the cross-section of the asynchronous railway traction motor is based on the aspects presented above. This optimization is justified with an example of: high-voltage three-phase squirrel cage asynchronous motor rated at: $P_N = 850$ kW—rated power; $U_N = 2500$ V—rated voltage; $I_{1N} = 223.4$ A—rated current; $f_1 = 80$ Hz—rated frequency; and $n_1 = 2400$ r.p.m.—synchronism speed.

The costs (fabrication, exploitation, and total) have been computed on the basis of the results obtained, taking into account that: $N_{ore} = 365 \times 10 = 3650$ h/year—yearly operation hours; $T_{ri} = 15$ years—period of the investment recovery; $c_{Cu} = 12$ €/kg—the cost of one kilo of copper; $c_{Fe} = 0.95$ €/kg—the cost of one kilo of iron (siliceous sheet); $c_{el.a} = 0.131$ €/kWh—the cost of one kWh of active electrical energy, and $c_{el.r} = 0.013$ €/kVARh—the cost of

one kVARhof reactive electrical energy. For the nominal data of the analyzed motor, using the design method known in the literature, a “reference motor” with the following costs resulted:

$$C_{f.m} = 29,750 \text{ €}; C_{e.m} = 317,000 \text{ €}; \text{ and } C_{t.m} = 346,700 \text{ €}.$$

All these results, obtained by the known design method, are considered reference quantities (for relating).

Restrictive conditions imposed have been as follows, gauge dimensions:

$$D_{ei} < 750 \text{ mm}, L_{ei} < 670 \text{ mm} \text{ and maximum torque: } m_{mi} = M_m / M_N > 2.4.$$

The graphics presented are plotted in per unit quantities. The costs are computed, in per unit quantities, with relations as follows:

$$c_t = \frac{C_{t \text{ var } m}}{C_{t m}} \quad c_f = \frac{C_{f \text{ var } m}}{C_{f m}}, \quad c_e = \frac{C_{e \text{ var } m}}{C_{e m}} \quad (11)$$

$C_{t \text{ var } m}$, $C_{e \text{ var } m}$, $C_{f \text{ var } m}$ are the total/exploitation/fabrication cost for the analyzed variant of motor;

$C_{t.m}$, $C_{e.m}$, $C_{f.m}$ are the total/exploitation/fabrication cost for the variant of motor considered as a reference.

4.1. Necessary Steps for Local Optimization in Relation to Each Variable

For each variable, local optimization is carried out by proceeding as follows:

- The relation for the resultant ampere-turn total (magneto-motive force for a pole pair) is considered, as known in literature:

$$U_{mm} = U_{m\delta} + U_{md1} + U_{mj1} + U_{md2} + U_{mj2} \quad (12)$$

$U_{m\delta}$ —air-gap magnetic voltage, U_{md1}/U_{md2} —stator/rotor tooth magnetic voltage, and U_{mj1}/U_{mj2} —stator/rotor yoke magnetic voltage;

- t.m.m. to the “reference motor” (the classically designed one) is calculated, and the obtained value will be kept constant during the optimization $U_{mm.i} = \text{const.}$;
- Each variable corresponds to at least one term of this sum, for example:
 - * For the variable D —the inner stator diameter, U_{mj1} , U_{md1} , U_{md2} , and U_{mj2} changes;
 - * For the variable D_i —the rotor lamination inner diameter, U_{mj2} changes;
 - * For the variable β_{c1} —the stator slot shape factor, U_{md1} and U_{mj1} changes;
 - * For the variable β_{c2} —rotor slot shape factor, U_{md2} and U_{mj2} , changes.

Local optimization in relation to a variable implies:

- The geometrical dimensions modify in the cross-section of the magnetic circuit; consequently, the afferent magnetic stresses are changed (magnetic field induction and intensity) for the established variable;
- The established variable is changed by $\pm 15\%$ compared to the known reference value, and the minimum value for U_{mm} —t.m.m. (rel. 12) is sought;
- B —the air-gap magnetic induction is progressively increased; consequently, all terms in the relation (12) increase, until the imposed value $U_{mm.i} = \text{const.}$ is reached;
- Thus, the optimum value of the analyzed variable is established.

Further, the procedure for the local optimization relative to the other variables is similar. Finally, for the values of the locally optimized variables, the relation (12) is re-considered, then U_{mm} is computed and, analogously, B is progressively increased until the imposed ampere-turn is obtained; $U_{mm.i} = \text{constant}$ in the motor optimization in relation sequentially to the four variables.

Non-linearity problems also appear in the optimization process; for example, $B = f(H)$ —the magnetization characteristic of the silicon sheet used in the construction of the magnetic circuit. In this case, the magnetic characteristic is given by a table with two lines (B and H) and n -columns (n —a large number of points to have a more accurate curve). At each

iteration, B —the magnetic induction in the calculation area (teeth or yoke, stator or rotor) is determined, and, through linear interpolation, we find H —the intensity of the magnetic field, required in the following calculations.

For the final optimal transversal geometry, it is necessary that these previously presented steps be repeated until the difference between these two consecutive optimal values is less than a predetermined error. A simultaneous optimization can be done considering all four variables, but the calculation program must be slightly modified.

4.1.1. Optimization Relative to Variable D (Motor Diameter)

The searching range imposed for this variable is a little bit affected by restrictions specific to railway traction: total length, Figure 3c and maximum torque, Figure 3d. In Figure 3a, the variation curves of the total ampere-turn for a pole pair are presented: U_{mm0} —for the optimized machine, U_{mm} —for the reference machine, and $U_{mm,i} = \text{const.}$ —for the “reference solemnity” imposed on the optimization.

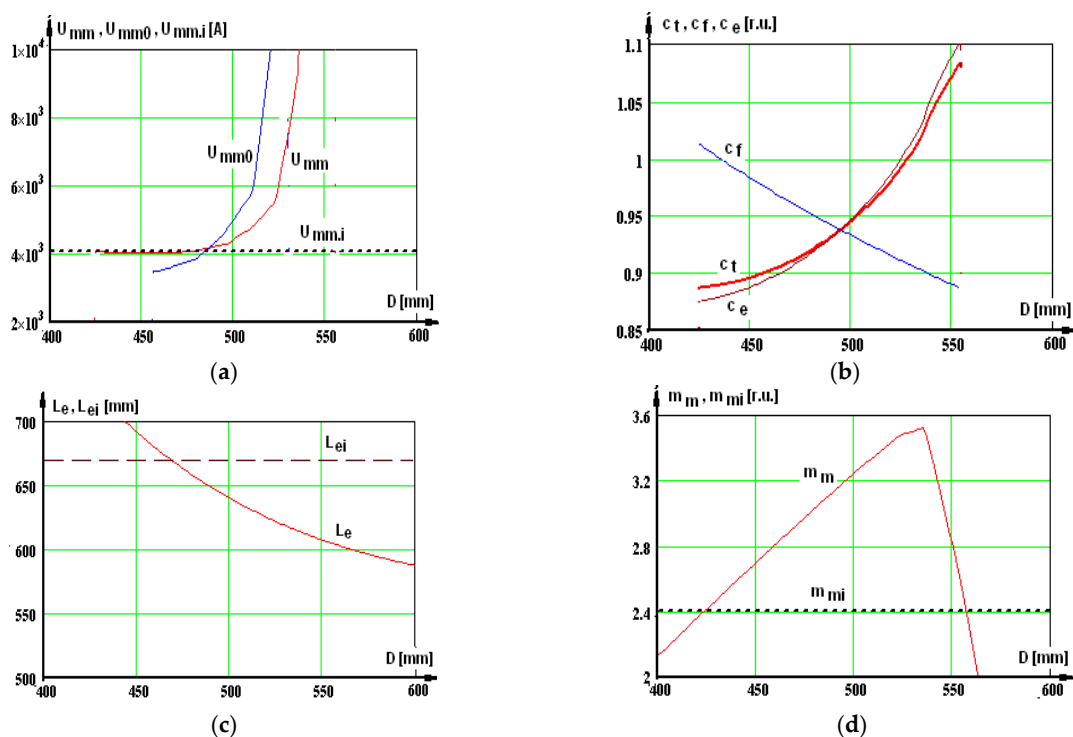


Figure 3. Variation curves relative to the variable D —machine diameter for: (a) total ampere-turn for a pole pair $U_{mm0}/U_{mm}/U_{mm,i}$ —for the optimized/real machine/imposed value; (b) $c_t/c_f/c_e$ —total/fabrication/exploitation cost; (c) total length; and (d) maximum torque.

The optimization results relative to the analyzed variable D are shown in Table 1. The optimum point resulted in $D = 460$ mm and, by optimization, resulted in an increase in the air-gap magnetic induction of the B value to 0.80 T and a decrease in the total cost with $\Delta c_t = 9.81\% = 34,000$ €.

Table 1. The values obtained for the analyzed case.

Variant	Criterion	C_t (€)	C_f (€)	C_e (€)	η	$\cos\varphi$	m_m (r.u.)
Values imposed		-	-	-	≥ 0.94	≥ 0.92	≥ 2.40
V_m —Real var.		346,700	29,750	317,000	0.951	0.923	2.648
V_o .—Opt. var.		312,700	28,930	283,800	0.956	0.926	2.807

4.1.2. Optimization Relative to the Variable D_{ir} (Rotor Inner Diameter)

Similar to the aspects presented above, the optimization relative to the variable D_{ir} is carried out. The results are not very spectacular, as seen in Table 2, which is why charts are not presented and discussed.

Table 2. The values obtained for the analyzed case.

Variant	Criterion	C_t (€)	C_f (€)	C_e (€)	η	$\cos\varphi$	m_m (r.u.)
	Values imposed	-	-	-	≥ 0.94	≥ 0.92	≥ 2.40
	V_m —Real var.	346,700	29,750	317,000	0.951	0.923	2.648
	V_o .—Opt. var.	346,300	29,060	317,200	0.951	0.920	2.682

The optimum point resulted in: $D_{ir} = 120$ mm and, by optimizing, there has been an increase in the air-gap magnetic induction to a value of $B = 0.708$ T and a decrease in the total cost with $\Delta c_t = 0.0894\% = 400$ €.

4.1.3. Optimization Relative to the Variable $\beta_{c1} = h_{c1}/b_{c1}$ (Stator Slot Shape Factor)

The optimization relative to this variable is important because there is a big difference between the curve of the existing motor, U_{mm} , and the curve of the optimized motor, U_{mm0} . Consequently, the magnetic induction may be much increased and the effect is a decrease in the total cost, as seen in Figure 4b. The restrictions, in Figure 4c,d, cause problems for small values of β_{c1} .

The results of the optimization relative to the analyzed variable β_{c1} , are shown in Table 3. The optimum point resulted in: $\beta_{c1} = 2.46$ and, by optimization, resulted in an increase in the air-gap magnetic induction to a value of $B = 0.707$ T and a decrease in the total cost, with $\Delta c_t = 2.596\% = 9000$ €.

Table 3. The values obtained for the analyzed case.

Variant	Criterion	C_t (€)	C_f (€)	C_e (€)	η	$\cos\varphi$	m_m (r.u.)
	Values imposed	-	-	-	≥ 0.94	≥ 0.92	≥ 2.40
	V_m —Real var.	346,700	29,750	317,000	0.951	0.923	2.648
	V_o .—Opt. var.	337,700	29,440	308,300	0.953	0.922	2.652

4.1.4. Optimization Relative to the Variable $\beta_{c2} = hc2/bc2$ (Rotor Slot Shape Factor)

In the case of this variable, which also defines the rotor slot geometry, there also occur differences, but small ones, between the curves U_{mm} and that of the optimized motor, U_{mm0} . Consequently, the magnetic induction can be increased a little bit and the effect is an increase in the total cost, as seen in Figure 5b. The torque restriction, as shown in Figure 5d, occurs for high values of β_{c2} .

The optimization results relative to the analyzed variable, β_{c2} , can be seen in Table 4. The optimum point resulted in a value of $\beta_{c2} = 6.2$ and, by optimization, has resulted in an increase in the air-gap magnetic induction so the value of $B = 0.70055$ T, a modification of the total cost by $\Delta c_t = -2.08\% = -7200$ €, indicating an increase in cost.

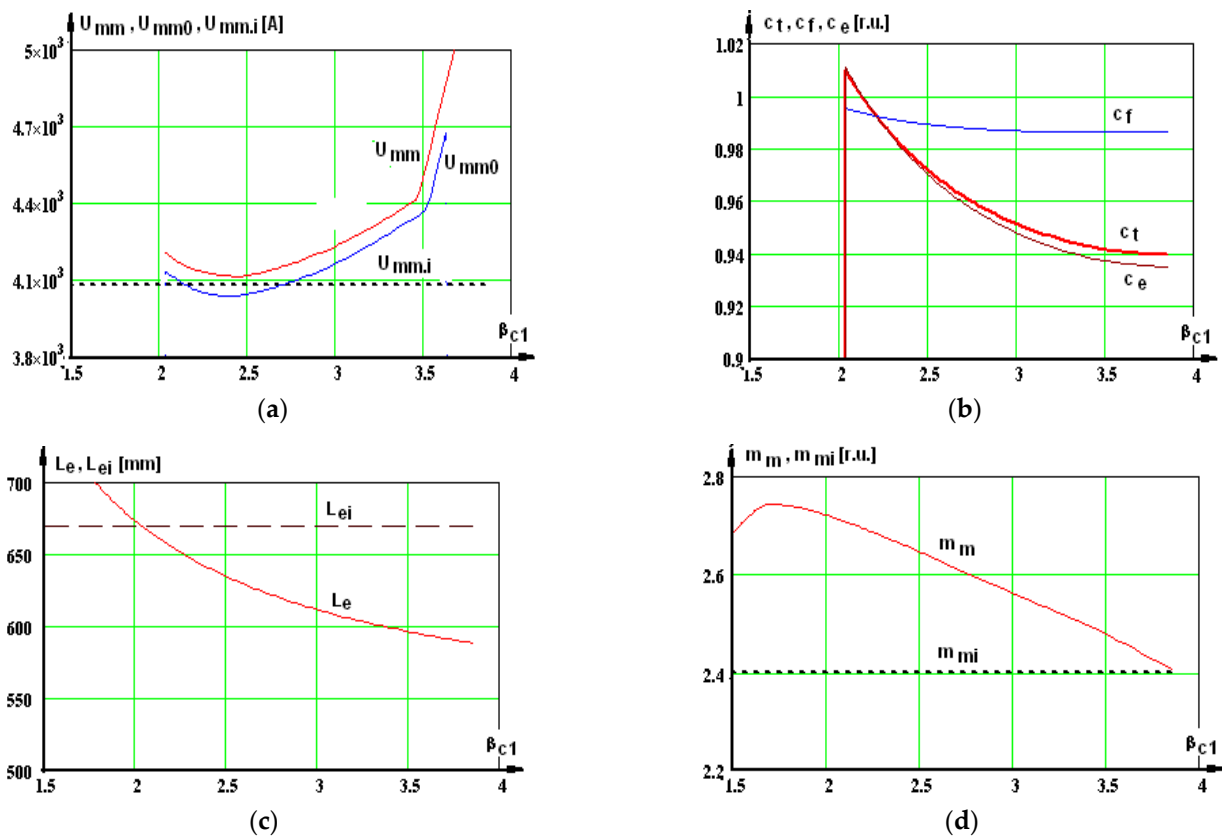


Figure 4. Variation curves relative to the variable β_{c1} —stator slot shape factor for: (a) total ampere-turn for a pole pair $U_{mm0}/U_{mm}/U_{mm,i}$ —for optimized/real machine/imposed value; (b) $c_t/c_f/c_e$ —total/fabrication/exploitation cost; (c) total length; and (d) maximum torque.

Table 4. The values obtained for the analyzed case.

Variant	Criterion	C_t (€)	C_f (€)	C_e (€)	η	$\cos\varphi$	m_m (r.u.)
Values imposed		-	-	-	≥ 0.94	≥ 0.92	≥ 2.40
V_m —Real var.		346,700	29,750	317,000	0.951	0.923	2.648
V_o —Opt. var.		353,900	30,180	323,700	0.950	0.917	2.402

4.1.5. The Final Optimal Solution for the Transversal Geometry of the Motor

On the basis of the optimization study carried out relative to the variables, the total optimization of traction motor cross geometry is approached, in which case, all four variables change simultaneously.

In the case of the analyzed motor, for the existing cross geometry, the results were $B = 0.71$ T (air-gap magnetic induction) and $U_{mm} = 4085$ A (ampere-turn for a pole pair).

For cross geometry optimization in relation to all variables, we aimed at preserving constant: total ampere-turn, $U_{mm} = 4085$ A; outer diameter, D_e ; and nominal power, P_N , and modifying the constructive dimensions of the stator and rotor lamination.

Thus, in the new geometry, in order to preserve the total ampere-turn at the proposed value, $U_{mm} = 4085$ A, the air-gap magnetic induction has been increased to the optimum value, $B_o = 0.868$ T, the results being shown in Table 5.

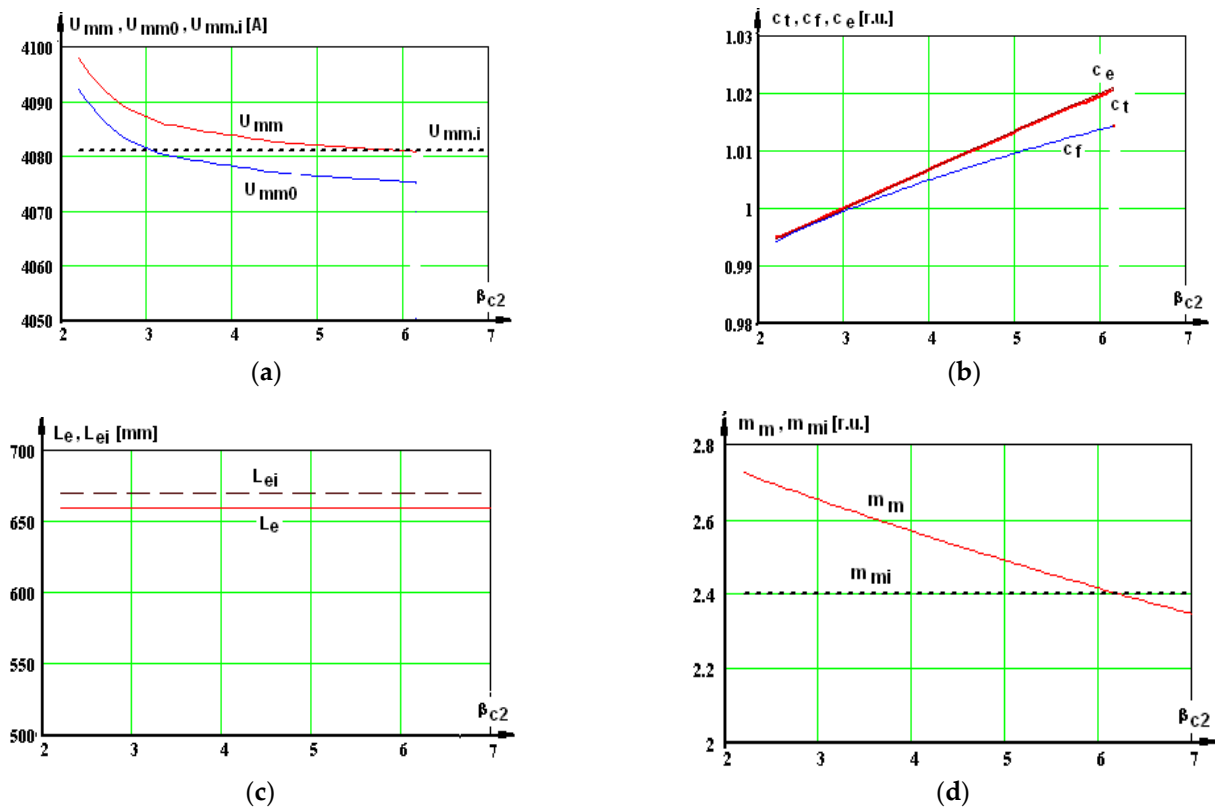


Figure 5. Variation curves relative to the variable β_{c2} —shape factor of the rotor slot for: (a) total ampere-turn for a pole pair $U_{mm0}/U_{mm}/U_{mm,i}$ —for the optimized machine/real machine/imposed value; (b) $c_t/c_f/c_e$ —total/fabrication/exploitation costs; (c) total length; and (d) maximum torque.

Table 5. Final optimum solution.

Variant	Criterion	C_t (€)	C_f (€)	C_e (€)	η	$\cos\varphi$	m_m (r.u.)
Values imposed		-	-	-	≥ 0.94	≥ 0.92	≥ 2.40
V_m —Real var.		346,700	29,750	317,000	0.951	0.923	2.648
V_o .—Opt. var.		304,100	27,930	276,200	0.957	0.920	2.934

It is noticeable, this time, that there is a significant decrease in the total cost in comparison with the motor considered as a reference, $\Delta c_t = 12.31\% = 42,600$ €, which indicates a very beneficial effect of the optimization.

Optimization can also be done in relation to the pairs of analyzed variables, but there are many combinations. We considered it sufficient to present only the final one, where all the variables appear.

5. Conclusions

The purpose of this research was to optimize the cross geometry of the asynchronous traction motor in the electrical locomotive.

We decided not to change the electrical stresses in considerations regarding the motor heating, preserving a constant total ampere-turn for a pole pair equal to that of the reference motor while maintaining the same air gap and using the same existing space efficiently (not changing the gauge dimensions).

The optimum cross geometry resulted in a decrease in the total cost by $\Delta c_t = 12.31\% = 42,600$ € because this constructive solution enabled an increase in the air-gap magnetic

induction of 22.25%, compared to the air-gap magnetic induction of the existing motor. If the asynchronous motor is used in an electrical locomotive where there are six traction motors, the total expenses decrease by $\Delta C_t = 6 \times 42,600 = 255,600$ €.

Author Contributions: Conceptualization, S.E. and I.V.; methodology, S.E.; software, I.V.; validation, S.E., I.V. and M.A.E.; and writing—review and editing, M.A.E. All authors have read and agreed to the published version of the manuscript.

Funding: University of Craiova.

Institutional Review Board Statement: Not applicable.

Informed Consent Statement: Not applicable.

Data Availability Statement: Not applicable.

Conflicts of Interest: The authors declare no conflict of interest.

References

1. Kreuawan, S.; Gillon, F.; Moussouni, F.; Brisset, S.; Brochet, P. Optimal design of traction motor in railway propulsion system. In Proceedings of the International Aegean Conference on Electric Machines, Power Electronics and Electromotion Joint Conference, Bodrum Turkey, 10–12 September 2007; pp. 343–348.
2. Abouzeid, A.F.; Guerrero, J.M.; Endemaño, A. Control strategies for induction motors in railway traction applications. *Energies* **2020**, *13*, 700. [[CrossRef](#)]
3. Finch, J.W.; Gsaoris, D. Controlled AC Electrical Drives. *IEEE Trans. Ind. Electron.* **2008**, *2*, 481–491. [[CrossRef](#)]
4. Fabrini, B.; Boldea, I. Electric Machinery and Adjustable Speed Motor Drives. Part I-Guest Editorial. *IEEE Trans. Ind. Electron.* **2007**, *5*, 2363–2364.
5. Chefneux, M.; Livadaru, L. *Solutions of Integrated Design of Electrical Machines for a Rational Use of the Natural and Artificial Resources*; CIT-TE-ICPE Publishing House: Bucharest, Romania, 2008.
6. Nigim, K.A.; DeLyser, R.R. Using MathCad in understanding the induction motor characteristics. *IEEE Trans. Educ.* **2011**, *44*, 165–169. [[CrossRef](#)]
7. Vlad, I.; Campeanu, A.; Enache, S. *Computer-Aided Design of Asynchronous Motors. Optimization Problems*; Universitaria Publishing House: Craiova, Romania, 2011.
8. *IEC 60034-2-1:2014*; Rotating Electrical Machines-Part 2-1. Standard Methods for Determining Losses and Efficiency from Tests. IEC: Geneva, Switzerland, 2014.
9. Boglietti, A.; Cavagnino, A.; Lazzari, M.; Pastorelli, M. International standards for the induction motor efficiency determination: A critical analysis of the stray load loss determination. *IEEE-IAS Trans. Ind. Appl.* **2004**, *40*, 1294–1301. [[CrossRef](#)]
10. Fasquelle, A.; Saury, D.; Harmand, S.; Randria, A. Numerical study of convective heat transfer in end region of enclosed induction motor of railway traction. *IJEET Int. J. Electr. Eng. Transp.* **2006**, *2*, 39–44.
11. Necula, D.; Vasile, N.; Stan, M.F. The Electrical Machines Impact on the Environment and Solution to reduce its. In *Scientific Bulletin of the Electrical Engineering Faculty*; Bibliotheca Publishing House: Târgoviște, Romania, 2011; pp. 37–42.
12. Maksay, S.T.; Stoica, D. *Computer-Aided Mathematics*; Politechnical Timisoara Publishing House: Timișoara, Romania, 2006. (In Romanian)
13. Campeanu, A.; Cautil, I.; Vlad, I.; Enache, S. *Modelling and Simulation of Alternating Current Machines*; Romanian Academy Publishing House: Bucharest, Romania, 2012.
14. Roux, P.F.; Ngwenyama, M.K. Static and Dynamic simulation of an induction motor using Matlab/Simulink. *Energies* **2022**, *15*, 3564. [[CrossRef](#)]
15. Samarkanov, D.; Gillon, F.; Brochet, P.; Laloy, D. Techno-economic optimization of induction machines: An industrial application. In Proceedings of the ACEMP—Electromotion 2011, Istanbul, Turkey, 8–10 September 2011; pp. 825–830.
16. Ta, C.M.; Chakraborty, C.; Hori, Y. Efficiency maximization of induction motor drives for electric vehicles based on actual measurement of input power. *Proc. IECON (IEEE-IES)* **2011**, *3*, 1692–1697.